Calorie Restriction Reduces the Influence of Glucoregulatory Dysfunction on Regional Brain Volume in Aged Rhesus Monkeys

Auriel A. Willette,[1,2,3] Barbara B. Bendlin,[1,3] Ricki J. Colman,[4] Erik K. Kastman,[1,3] Aaron S. Field,[5] Andrew L. Alexander,[2] Aadhavi Sridharan,[1,3,6] David B. Allison,[7] Rozalyn Anderson,[1,4] Mary-Lou Voytko,[8] Joseph W. Kemnitz,[4,9,10] Richard H. Weindruch,[1] and Sterling C. Johnson[1,2,3,4,6]

Insulin signaling dysregulation is related to neural atrophy in hippocampus and other areas affected by neurovascular and neurodegenerative disorders. It is not known if long-term calorie restriction (CR) can ameliorate this relationship through improved insulin signaling or if such an effect might influence task learning and performance. To model this hypothesis, magnetic resonance imaging was conducted on 27 CR and 17 control rhesus monkeys aged 19–31 years from a longitudinal study. Voxel-based regression analyses were used to associate insulin sensitivity with brain volume and microstructure cross-sectionally. Monkey motor assessment panel (mMAP) performance was used as a measure of task performance. CR improved glucoregulation parameters and related indices. Higher insulin sensitivity predicted more gray matter in parietal and frontal cortices across groups. An insulin sensitivity × dietary condition interaction indicated that CR animals had more gray matter in hippocampus and other areas per unit increase relative to controls, suggesting a beneficial effect. Finally, bilateral hippocampal volume adjusted by insulin sensitivity, but not volume itself, was significantly associated with mMAP learning and performance. These results suggest that CR improves glucose regulation and may positively influence specific brain regions and at least motor task performance. Additional studies are warranted to validate these relationships.
***Diabetes* 61:1036–1042, 2012**

Lower insulin sensitivity and reduced insulin-mediated glucose uptake can adversely impact the brain. Glucoregulatory dysfunction is related to less gray matter (GM) volume cross-sectionally and longitudinally in medial temporal lobe, prefrontal cortex, and other areas impacted by normal aging, neurovascular disorders, and Alzheimer disease (AD). Such relationships are seen in both rhesus monkeys (1) and humans (2,3). Importantly, insulin-signaling dysfunction in AD patients can negatively influence brain volume in the absence of type 2 diabetes (3), suggesting that mild to moderate glucoregulatory perturbation may be detrimental over time. Studies in rodents show that medial temporal lobe and prefrontal cortex have dense insulin receptor staining and may rely on insulin signaling for optimal glucose uptake and utilization (2,4). AD is characterized by reduced insulin sensitivity, transcription of mitochondrial metabolism genes, and central glucose uptake (5,6). Lower insulin sensitivity may pathogenically affect the brain through microvascular disease (7), increased production of advanced glycation end products and free radicals (8,9), or lower cerebral blood flow and glucose transport (10).

Despite these relationships between insulin signaling and brain, studies vary widely in the glucoregulatory measures and brain areas that are assessed (11). It is therefore of interest to use voxel-wise analysis methods (12) to investigate where insulin sensitivity variation is associated with regional volume or tissue microstructure across the brain. Our group has previously reported on the longitudinal effects of calorie restriction (CR) regarding glucose regulation in aged rhesus macaques since middle age (13–15). CR led to improved glucose tolerance and higher insulin sensitivity, effects that may benefit areas like hippocampus and prefrontal cortex and mediate improved task learning and performance. This cohort therefore afforded a unique opportunity to look at the effects of CR on glucose regulation and its association with brain and behavior in a primate species.

In this study, an index of insulin sensitivity, S_I, was derived from a glucose tolerance test. This measure represents the ability of insulin to promote glucose uptake and inhibit hepatic glucose production (13,16). Insulin sensitivity in the periphery and brain strongly correspond (17). We hypothesized that higher S_I would predict more GM volume in brain areas with dense insulin receptor staining and that are affected by insulin signaling dysregulation (2,18–21). Furthermore, it has been well established that CR in nonhuman primates has several beneficial effects related to glucose regulation, such as improved vascular health, lower triglycerides, and other factors that delay age-associated pathogenesis (22). Thus, we tested the interaction between S_I and dietary condition, to see if CR monkeys exhibited more volume or tissue density per S_I unit increase versus controls beyond the association between S_I and brain seen across both dietary groups. In other words, this interaction tested if there was a region-specific beneficial effect for restricted animals. Several

From the [1]Geriatric Research Education and Clinical Center, William S. Middleton Memorial Veterans Hospital, Madison, Wisconsin; the [2]Waisman Laboratory for Brain Imaging and Behavior, University of Wisconsin-Madison, Madison, Wisconsin; the [3]Wisconsin Alzheimer's Disease Research Center, University of Wisconsin School of Medicine and Public Health, Madison, Wisconsin; the [4]Wisconsin National Primate Research Center, Madison, Wisconsin; the [5]Department of Radiology, University of Wisconsin-Madison, Madison, Wisconsin; the [6]Neuroscience Training Program, University of Wisconsin-Madison, Madison, Wisconsin; the [7]Department of Biostatistics, University of Alabama at Birmingham, Birmingham, Alabama; the [8]Department of Neurobiology and Anatomy, Wake Forest School of Medicine, Winston-Salem, North Carolina; the [9]Department of Cell and Regenerative Biology, University of Wisconsin School of Medicine and Public Health, Madison, Wisconsin; and the [10]Institute for Clinical and Translational Research, University of Wisconsin-Madison, Madison, Wisconsin.
Corresponding author: Sterling C. Johnson, scj@medicine.wisc.edu.
Received 8 September 2011 and accepted 11 January 2012.
DOI: 10.2337/db11-1187
© 2012 by the American Diabetes Association. Readers may use this article as long as the work is properly cited, the use is educational and not for profit, and the work is not altered. See http://creativecommons.org/licenses/by-nc-nd/3.0/ for details.

insulin signaling, glycation, and vascular measures were tested as potential mediating factors (1,8). Finally, due to hippocampus being susceptible to glucoregulatory dysfunction (3) and its role in AD, we performed a region of interest (ROI) analysis limited to that region. The ROI analysis, which was independent from the voxel-wise results (23), tested the extent to which predicted changes in hippocampus specific to S_I were associated with visuomotor performance on the monkey motor assessment panel (mMAP) (24,25). The hippocampus is in part involved in learning new spatiomotor sequences (26).

RESEARCH DESIGN AND METHODS

Subjects. Forty-four rhesus monkeys (*Macaca mulatta*) between 19 and 31 years of age were included in this study. Seventeen animals were fed ad libitum for approximately 8 h/day, whereas the remaining 27 subjects were fed 30% fewer calories relative to their own baseline intake. Length of CR diet was 12–17 years and initiated in middle age. Demographic data are available in Table 1. These monkeys were the remaining subjects of a longitudinal CR project begun at the Wisconsin National Primate Research Center in 1989. Details of the CR manipulation, housing, and husbandry have been described previously (13,27).

Magnetic resonance imaging data acquisition and preprocessing. Scan session and image acquisition parameters have been detailed elsewhere (28). Briefly, animals were anesthetized while images were acquired using a General Electric 3.0 T scanner (GE Medical Systems, Milwaukee, WI). T1-weighted volumetric scans were used to determine regional volumes. Diffusion tensor imaging was acquired to quantitatively estimate coherence of white matter tracts by computing fractional anisotropy, axial diffusivity, and radial diffusivity, whereas microstructural density of brain parenchyma was determined using mean diffusivity (29). T1-weighted scan parameters were: repetition time = 8.772 ms; echo time = 1.876 ms; inversion time = 600 ms; flip angle = 10°; number of excitations = 2; matrix = 256 × 224; and field of view = 160 mm. A total of 124 coronal slices were acquired with a thickness of 0.7 mm and no gap, resulting in 0.625 × 0.625 × 0.7 mm voxels. For diffusion tensor imaging, a diffusion-weighted echo-planar imaging sequence with 12 gradients was used with the following parameters: repetition time/echo time = 10,000/77.2 ms; b = 816 s/mm^2; number of excitations = 6; field of view = 140 mm; in-plane matrix = 256 × 256; and slice thickness = 2.5 mm, no gap, and 35 slices. Voxels were resampled to 0.5 × 0.5 × 0.5 mm for T1-weighted and diffusion tensor imaging sequences. T2-weighted scans were acquired for global volume estimation and are described elsewhere (28).

Imaging artifacts. All images were inspected to locate scan artifacts that could adversely affect the voxel-wise analyses. Three diffusion tensor-imaging scans and one volumetric scan had artifact abnormalities (motion, respiratory, phase, other) or gross misregistration with the template brain that rendered data unusable. Six additional diffusion tensor-imaging scans (controls = 2, CR = 4) had one or more 1- to 2-mm abnormalities located in the white matter of the dorsal convexity that precluded analysis.

Magnetic resonance imaging preprocessing. Preprocessing of magnetic resonance images for use in voxel-wise analyses has been described previously (28,30). Briefly, T1-weighted images were segmented and normalized to 112RM-SL atlas space (28) with Diffeomorphic Anatomical Registration Through Exponentiated Lie algebra (31). Volumetric segments were smoothed using a 4-mm full width at half maximum Gaussian kernel. Fractional anisotropy, mean diffusivity, axial diffusivity, and radial diffusivity maps were computed using DTIFIT in FSL (www.fmrib.ox.ac.uk/fsl/). Diffusion tensor-imaging measurements were aligned to the 112RM-SL atlas space in SPM and smoothed with a 4-mm smoothing kernel.

Glucoregulation and other physiological indices. We have previously described the frequently sampled glucose tolerance test procedure that provides data on basal and acute glucose and insulin signaling dynamics (13). Derived indices relevant to this report are described in Table 1. Glucoregulation measures were collected within 6 months of the magnetic resonance imaging (MRI) scan. Insulin sensitivity, or S_I, was calculated using the Minimal Method Model (32). This measure provides an accurate quantification of S_I, as well as other aspects of glucose kinetics, and is far more practical than other methods like the glucose-clamp technique. Plasma glucose was measured using the glucose oxidase method (Yellow Springs Instruments, Yellow Springs, OH). Insulin levels were determined using double antibody radioimmunoassay (Millipore, Billerica, MA). The homeostatic assessment of insulin resistance (HOMA-IR) was calculated using basal glucose and basal insulin (33). HOMA-IR was calculated in order to see if basal insulin resistance explained variance beyond its converse construct, which would be insulin sensitivity measured by S_I. Homocysteine was collected using methods previously described (30). Glucoregulatory data near the time of the MRI scan were not available for one CR and one control monkey.

Glucoregulatory impairment. Animals were classified by an expert (R.J.C.) as having normal, prediabetic/at-risk, or type 2 diabetes-like profiles using established criteria (15).

Anatomical region of interest: hippocampus. In order to independently assess (23) if glucoregulatory dysfunction might influence motor learning via S_I predicted variation in brain, an expert (A.A.W.) drew a mask on the 112RM-SL atlas to isolate the bilateral hippocampus using methods previously described (34). Mean GM volume was extracted from the ROI for all normalized monkey brains and was used in conjunction with S_I to predict performance on a motor task described next.

Motor learning and performance. It was of interest to see if the relationship between insulin signaling and hippocampal volume predicted changes in motor task learning and performance. To this end, our cohort has previously been tested on the mMAP (25), which required subjects to retrieve an appetitive stimulus from a flat platform, straight rod, or curved rod (24). An automated system recorded the number of seconds necessary to reach from the home cage to the first area of the affixed apparatus (reaction time), from the first to second area (coarse motor movement), and from the second area to a small receptacle that held the stimulus (fine motor movement). We used fine motor performance data from the most difficult task (i.e., curved rod), because CR animals acquire and perform this task more quickly than controls (25). Animals did not differ on simpler tasks. To test our hypothesis regarding insulin signaling and hippocampal volume, these performance measures were correlated with hippocampal volume adjusted or not adjusted by S_I. The sample size for this analysis was 26 animals (C = 7; CR = 19).

Voxel-wise statistical analyses: structural MRI. To investigate regional brain associations of S_I, multiple regression voxel-wise analyses were conducted in SPM8 (12). For the purposes of this report, this type of regression technique produces *t*-statistic, color-coded result maps that are the product of a regression model performed at every voxel in the brain for a given modality. Contiguous groups of voxels that attain statistical significance, called clusters, will thus overlap with and implicate different brain regions. In this study, volumetric or diffusion tensor-imaging scans were entered as the dependent variable. The independent variable was S_I. Covariates included age at scan, sex, dietary condition, and the S_I term when testing an interaction (see below). Analyses of volume additionally covaried a global index of either gray or white matter (28). Our primary analysis of interest was testing a S_I × dietary condition interaction term to see if CR monkeys showed more volume or microstructure per S_I unit change beyond the association seen with S_I alone, suggesting a further beneficial effect. The voxel and cluster level thresholds were set at $P < 0.005$ (uncorrected) and $P < 0.05$ (corrected). Type 1 error was minimized by first using an omnibus F-contrast ($P < 0.05$, uncorrected) for S_I, dietary condition, and S_I × dietary condition to mask subsequent contrasts, followed by Monte Carlo simulations to estimate cluster sizes that would occur due to chance (25,30). Clusters required 280 contiguous voxels to reach significance at $P < 0.05$ (corrected). Reported whole-brain cluster coordinates correspond to the Saleem-Logothetis atlas (35) and are displayed on the 112RM-SL template image (28). Standard rhesus monkey atlases were used to identify fibers (36) and subcortical structures (37).

Statistical analyses: brain-physiology and brain-behavior associations. Tests were conducted using SPSS 18.0 (SPSS Inc., Chicago, IL) at an α of 0.05. Logarithmic transformations were used to adjust nonnormally distributed indices. ANOVA tested group differences for demographic and biological variables. Multiple regression was used to determine which basal and frequently sampled glucose tolerance test variables significantly explained error variance in the S_I association and interaction voxel-wise analyses. The first regression block included HOMA-IR to account for basal insulin regulation. The second block contained a priori variables of interest directly related to S_I: basal glucose and insulin, compensatory pancreatic sensitivity represented by Disposition Index (13), and glycosylated hemoglobin levels. The third block contained the vascular risk factor homocysteine.

Brain-behavior mediational models tested whether or not S_I-predicted variation in brain was correlated with motor learning and performance. To avoid circular analysis (23), an independent anatomical ROI approach was used to derive mean image signal (e.g., mean GM volume) within the bilateral hippocampus. S_I was then linearly regressed onto the hippocampal signal. The Pearson's statistic was then used to correlate the predicted change in hippocampal volume due S_I with the mean number of seconds it took for a monkey to complete the fine motor portion of the curved rod mMAP task during initial acquisition (i.e., the learning phase) and when the animal reached proficiency (25).

RESULTS

Subject characteristics and biological indices. See Table 1 for descriptive data and statistics. The mean age, sex composition, and total brain volume of the two dietary

TABLE 1
Demographics, total brain volume, and glucoregulatory values for control and CR monkeys

	Control	Range	CR	Range	*P* value
Demographics and global volume					
Age (years)	23.84 ± 2.79	19–27	24.32 ± 2.77	19–31	NS
Sex (male/female) (*n*)	7/10	NA	11/16	NA	NS
Body weight (kg)	12.39 ± 2.84	9–19	8.94 ± 1.71	6–12	0.001
Total brain volume (mm^3)	86.80 ± 10.56	67–105	82.45 ± 9.20	56–99	NS
Physiological indices					
Basal glucose (mg/dL)	82.56 ± 41.77	52–218	60.78 ± 7.44	51–82	0.009
Basal insulin (μU/mL)	47.81 ± 50.47	4–199	19.26 ± 17.93	4–82	0.009
Disposition Index ($[\Delta I_{(0-30)}/\Delta G_{(0-30)}]/I_b$)	1,931 ± 1,521	138–5,705	4,244 ± 2,411	106–12,483	0.001
HbA_{1c} (%)	10.48 ± 4.41	7–22	8.59 ± 1.56	5–12	0.043
Homocysteine (μmol/L)	8.16 ± 3.30	5–15	9.88 ± 5.09	5–24	NS
HOMA-IR ($[G_b \times I_b]/405$)	8.62 ± 7.63	0.51–28	2.99 ± 2.86	0.50–12	0.001
S_I ($\mu U/mL \times 10^4\ min^{-1}$)	3.28 ± 2.31	0.23–7	7.44 ± 4.11	0.61–16	0.001

The unit of measurement, mean ± SD, and range for a given variable is noted for control and then CR monkeys. Insulin sensitivity, as assessed by S_I, quantitatively represents the capacity of insulin to stimulate glucose uptake and inhibit glucose production. Disposition Index represents pancreatic insulin sensitivity and is calculated as the ratio of insulin secretion to glucose uptake 0–30 min after glucose bolus as compared with prechallenge insulin levels. Basal glucose, basal insulin, and HOMA-IR are based on samples collected before glucose bolus administration. Glucoregulatory data besides basal measures near the time of scan were not available for one CR and one control monkey. ANCOVA was used to test for dietary group effects.

conditions did not differ. CR monkeys showed expected benefits in insulin signaling and related indices (22).

Prediabetic and diabetic glucoregulatory impairment. Six controls and zero CR monkeys were classified as having preclinical ($n = 4$) or diabetes-like glucoregulatory dysfunction ($n = 2$). Diagnosis was not a significant covariate in regression analyses.

Regional GM: S_I association. To examine the association of S_I on regional GM, S_I was regressed onto GM volume voxels across all subjects. As indicated in Fig. 1*A–C* (yellow-orange areas) and Table 2, higher S_I predicted more GM in motor and somatosensory cortices. Fig. 1*G* depicts this relationship by illustrating the correlation between S_I and the voxel with the highest (peak) *t*-statistic located in left primary motor cortex. The association of S_I and GM was comparable for both control ($R^2 = 0.516$; $P < 0.001$) and CR ($R^2 = 0.324$; $P < 0.001$) monkeys.

Regional GM: predictors of S_I association. Measurements directly or indirectly related to glucoregulation that are described in Table 1 may elucidate potential mechanisms underlying the relationship between S_I and regional GM. Therefore, follow-up multiple linear regression was conducted. The dependent variable was the predicted volume change in left motor cortex shown in Fig. 1*G*. Different regression models using stepwise, forward, or enter methods produced similar results (data not shown). The final adjusted regression model predicted 20.7% of the variance across both groups [$F(6,35) = 4.170$; $P < 0.01$]. Although the influence of S_I on GM was not significantly mediated by HOMA-IR or basal glucose, increased basal insulin was modestly related to less GM ($R^2 = 0.133$; $P < 0.05$). Higher levels of homocysteine ($R^2 = 0.169$; $P < 0.05$) and glycosylated hemoglobin ($R^2 = 0.148$; $P < 0.05$) were also associated with less frontal GM volume.

Regional GM: S_I × dietary condition. Given the salubrious effects of CR on vascular health and metabolic indices related to improved glucose regulation (22), we tested for a similar beneficial effect on the brain in CR monkeys. Thus, this contrast examined if CR monkeys had more GM volume per unit increase in S_I compared with controls beyond the association with S_I alone, suggesting a protective effect. As shown in Table 2 and depicted in Fig. 1*A* (purple areas), voxel clusters were present in bilateral anterior hippocampus and both inferior and middle temporal gyri. The interaction is represented in Fig. 1*H* using the peak *t*-statistic voxel. CR monkeys showed more GM as S_I increased ($R^2 = 0.159$; $P < 0.05$). For controls, however, higher S_I unexpectedly corresponded to less GM ($R^2 = 0.449$; $P < 0.01$). To validate this result, a mean index of S_I was calculated using data from all glucose tolerance tests since the start of the project in 1989, which was up to 14 assessments depending on the length of time an animal spent in the study. This index or area under the curve estimates resulted in clusters and graphs similar to those produced using the S_I value nearest to the MRI scan date (data not shown). Additional significant brain areas found in the interaction analysis were caudal perirhinal, entorhinal, and parahippocampal cortices, insula, amygdala, temporal pole, anterior cingulate cortex, and orbital and medial prefrontal cortices (Fig. 1*A–F*).

Regional GM: predictors of S_I × dietary condition effect. Multiple linear regression was simultaneously performed on each dietary condition group to detect mediators that might explain the S_I × dietary condition interaction effect. The dependent variable was the predicted change in hippocampal GM depicted in Fig. 1*H*. The same regression model was used as in the S_I association analysis (see RESEARCH DESIGN AND METHODS). Table 3 indicates the result. Fig. 2*A–C* shows that control monkeys had strong associations between HOMA-IR, basal insulin, or basal glucose and GM related to the interaction. Fig. 2*D–F* shows nonsignificant relationships for the same variables in CR monkeys.

S_I predicted variation in hippocampus GM and fine motor performance. We finally wished to test if predicted changes in hippocampal GM related to S_I were associated with mMAP fine motor performance during the curved rod task (24). An independent analysis was conducted using S_I measured at the time closest to scan in 7 controls and 19 CR monkeys that had successfully learned the task. As reported elsewhere (25), this task was chosen because CR monkeys performed it significantly more quickly during acquisition (CR: 4.84 s; control: 6.26 s) and after gaining proficiency (CR: 3.08 s; control: 3.73 s).

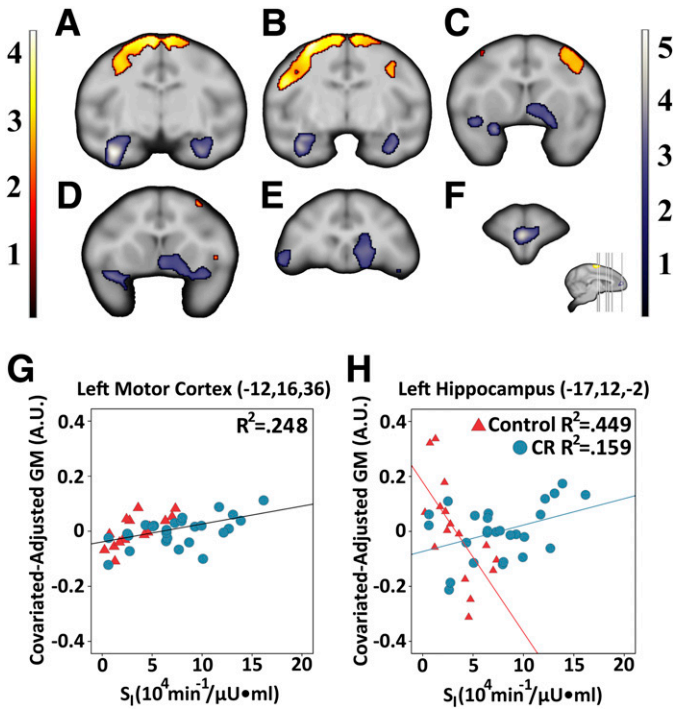

FIG. 1. The relationship between S_I and regional GM volume across subjects and an S_I × dietary condition interaction testing such an association for each dietary group. S_I near the time of scan was not available for one control and one CR monkey. Sixteen controls and 26 CR monkeys were analyzed. Higher S_I for both control and CR monkeys (yellow-orange color) corresponded to more GM in parietal and frontal cortices (*A–C*). For the interaction, CR animals showed more GM per unit increase in S_I compared with controls in hippocampus, temporal pole, agranular insula, striatum, prefrontal cortices, and anterior cingulate cortex (purple color, *A–F*). To illustrate these results, a representative voxel from each analysis was graphed, both for the association of S_I across groups (*G*) and the interaction between groups (*H*). A sagittal view of the brain depicts the location of the coronal slices in *A–F* along a posterior-anterior axis. Color bars and color maps represent *t* values. GM volume is depicted in arbitrary units (A.U.). Brains are oriented such that the left hemisphere is on the left side.

Unadjusted hippocampal volume was not related to motor learning (R^2 = 0.034; not significant) or proficient (R^2 = 0.01; not significant) mMAP performance. By contrast, when first adjusting hippocampal volume by S_I, this brain measure significantly explained 12% of the variance for mMAP performance during the acquisition phase (P = 0.042) and 24.1% (P = 0.005) after monkeys became proficient at the task (25).

Regional white matter, diffusion tensor imaging, and S_I analyses. No clusters exceeded the minimum number of voxels required for type 1 error correction in white matter volume or diffusion tensor imaging modalities.

DISCUSSION

We hypothesized that higher insulin sensitivity, indexed by S_I, would predict more GM or denser microstructure in brain regions that are influenced by insulin signaling and impacted by neurodegenerative and neurovascular disorders. Across CR and control subjects, higher S_I was associated with more GM volume in somatosensory and motor cortices. These areas have low insulin receptor density relative to medial temporal lobe and prefrontal cortex in rodents (38). Interestingly, S_I interacted with dietary condition, for which CR monkeys with higher S_I had significantly more GM in hippocampus, insula, prefrontal cortex, and other regions with a high density of insulin receptors. Higher S_I among controls was unexpectedly related to less GM in these regions. Models suggest that prediabetes or type 2 diabetes in controls did not influence this result. Similar relationships between impaired glucoregulation and brain volume have been seen in AD patients with no history of type 2 diabetes (3). As such, mild to moderate insulin signaling dysregulation may negatively affect key brain areas.

Although the relationship between S_I and GM among controls in the interaction was unexpected, it is not likely due to assay error or a sudden change in glucoregulatory dynamics. A similar interaction result was found when using a mean S_I index derived from every glucose tolerance test conducted since 1989. More importantly, an estimate of basal insulin resistance, HOMA-IR, corresponded to less hippocampal GM in controls, a result that has been observed in humans (21). No relationship was seen between S_I and white matter volume or tissue microstructure, which may reflect the role of insulin-like growth factor signaling rather than insulin in mediating oligodendrocyte development and growth factor-mediated preservation (39). Although tissue microstructure is negatively impacted by type 2 diabetes (40), it may be due to vascular pathology or other consequences instead of antecedent decreases in insulin sensitivity.

Our results suggest that there is wide variation in how insulin signaling may affect energy metabolism and other functions in brain. The central action of insulin on reducing oxidative damage or maintaining synaptic plasticity appears to be area-specific due to receptor density and binding dynamics (2,17,38). For example, intracerebrovascular treatment of rats with low doses of streptozotocin, which is normally toxic to pancreatic insulin-secreting cells and creates a diabetes-like state, reduced downstream phosphatidylinositol-3 kinase activity primarily in hippocampus but to a much lesser extent in frontal cortex without affecting peripheral glucose regulation (41). Intracerebrovascular administration of insulin also affected adenosine 5′-triphosphate storage in hippocampus but not parietotemporal cortex (4).

By extension, the relatively moderate relationship between higher S_I and more GM in motor and somatosensory areas may be due to indirect mechanisms attributed to higher insulin concentrations. Chronic peripheral hyperinsulinemia is typically characterized by hyperglycemia and breakdown of the epithelial vasculature. Levels of glycosylated hemoglobin and homocysteine, a biomarker for vascular health, were significant mediators of the association between S_I and GM. In brain, it is conceivable that a microvascular insult combined with other neuropathologies might synergistically reduce perfusion and glucose transport into parenchyma, leading to damage (42). For example, streptozotocin alone in transgenic APP/PS1 mice produced more advanced glycation end products in microvasculature and worse spatial performance; similar pathophysiological effects were also seen in human cerebromicrovascular cells exposed to streptozotocin and amyloid β (9).

The interaction of S_I and GM between dietary groups revealed several important findings related to insulin signaling and brain in CR versus control monkeys. Ameliorative effects may be due to the direct action of insulin, although CR may act through related mechanisms such as less atherogenic dyslipidemia, lower expression of

TABLE 2
Voxel-wise results for S_I and GM volume

Location	x, y, z	t	Cluster size (voxels)
S_I association			
L primary motor cortex	−12, 16, 36	4.38	7,538
L somatosensory areas 3a and 3b	−22, 16, 23	3.88	
L primary motor cortex	−3, 12, 38	3.86	
R primary motor cortex	18, 19, 30	3.20	2,007
S_I × dietary condition interaction			
L hippocampus	−17, 12, −2	5.37	3,025
L medial prefrontal cortex	−2, 44, 17	4.80	1,332
R ventral prefrontal cortex	6, 38, 20	3.14	
L dorsal inferotemporal cortex	−28, 6, 8	4.52	1,842
R hippocampus	14, 13, −1	3.85	1,827
L agranular temporal pole	−12, 24, 4	3.84	847
L medial belt of auditory cortex	−21, 20, 5	3.06	
R striatum	7, 31, 14	3.51	3,602
R agranular insula	14, 28, 5	3.37	
R orbital prefrontal cortex	1, 26, 10	3.29	
L primary visual cortex	−11, −20, 30	3.47	320
L ventral prefrontal cortex	−24, 32, 10	3.44	393

The relationship between an index of insulin sensitivity, S_I, and GM volume across subjects (S_I association) and between the control and CR groups (S_I × dietary condition interaction). For a given voxel-wise analysis, a given term was regressed onto each GM voxel in the brain. The voxel threshold for statistical significance was $P < 0.005$. Type 1 error was minimized when considering groups of contiguous, statistically significant voxels called clusters in different brain regions. Specifically, using Monte Carlo simulations, clusters had to exceed a number of voxels (cluster size) such that clusters generated from the data had a $P < 0.05$ of occurring by chance. For larger clusters, results are displayed for the maximally significant voxel followed by voxels from nearby regions. Coordinates refer to the sagittal, coronal, and axial planes of the Saleem-Logothetis atlas for rhesus macaques. L, left; R, right.

proinflammatory cytokines, and fewer prothrombotic factors due to reduced insulin resistance (43). S_I represents the capacity for insulin to facilitate glucose uptake and inhibit hepatic production. Lower S_I would correspond to a higher insulin secretion peak followed by prolonged hyperinsulinemia. In this vein, Burns and coworkers (3) found that a higher insulin area under the curve during a glucose tolerance test predicted more hippocampal GM in early AD without a history of type 2 diabetes, but not in nondemented participants. This compensatory response may reflect glucoregulatory and metabolic dysfunction that can occur in early AD (2,6). Similarly, mediational models suggest that control animals with high basal insulin, but relatively lower basal glucose levels, would benefit from reduced insulin sensitivity in areas that rely on insulin signaling for optimal neural function. Previous studies have shown that infusion of insulin or antagonism via streptozotocin affects adenosine 5′-triphosphate storage in hippocampus (4), dopamine metabolism in striatum (44), and 2-deoxy-D-[^{14}C]glucose utilization in rat medial temporal lobe, striatum, and frontal cortex (18). All of these brain regions were implicated in the current study. Although this compensatory mechanism for rhesus monkey controls may benefit these areas, hyperinsulinemia and lower insulin sensitivity is harmful to skeletal muscle (45) and may also cause vascular damage (42).

CR monkeys showed the expected relationship between higher S_I and more GM in the S_I × dietary condition interaction. This positive correlation was similar to CR results for the S_I association analysis. We have previously established that CR in rhesus monkeys reduced basal glucose and insulin, lowered insulin resistance, and increased lean muscle intracellular receptor substrate-1 expression (14,46). Such effects for glucoregulatory indices were also found in the current sample. Either intermittent fasting or CR also lowers serum glucose and insulin, as well as protects hippocampal neurons from excitotoxic injury induced by kainite (47).

Finally, hippocampal GM volume adjusted by S_I was significantly correlated with learning and memory performance for the mMAP task, whereas there was no relationship with unadjusted volume. This analysis was independent from voxel-wise analyses to minimize circularity concerns (23). Both approaches are complementary and can elucidate potential relationships among

TABLE 3
Significant predictors of SI × dietary condition interaction with regional GM

Dietary condition	Variable	B	SE b	β	t
	Constant	1.889	0.412		
	HOMA-IR	−0.013	0.004	−0.526*	−3.097
	DI	−3.515E-5	1.069E-5	−0.286†	−3.284
Control	I_b	0.402	0.067	0.877‡	5.990
	G_b	−1.780	0.248	−0.969‡	−7.185
	HbA_{1c}	1.000	0.132	0.794‡	7.589
	Homocysteine	0.011	0.009	0.198	1.194
	Constant	0.053	0.833		
	HOMA-IR	0.017	0.019	0.502	0.905
	DI	9.296E-6	9.018E-6	0.229	1.031
Calorie restriction	I_b	−0.169	0.178	−0.539	−0.539
	G_b	0.125	0.492	0.064	0.064
	HbA_{1c}	−0.182	0.282	−0.150	−0.150
	Homocysteine	−0.001	0.005	−0.037	−0.156

Multiple regression was used to assess which glucoregulatory variables from a frequently sampled glucose tolerance test mediated the S_I × dietary condition interaction effect. Specifically, using data from a representative voxel in left anterior hippocampus, glucoregulatory measures were regressed onto the predicted change in GM due to insulin sensitivity for control or CR monkeys. For the final control model, the adjusted R^2 of the mediation model was 0.889 [$F(4,15) = 25.137$; $P < 0.001$]. For the final CR mediational model, the adjusted R^2 was 0.142 [$F(5,25) = 0.378$; NS]. DI, Disposition Index; G_b, basal glucose; HbA_{1c}, glycosylated hemoglobin; I_b, basal insulin. *$P \leq 0.05$. †$P < 0.01$. ‡$P \leq 0.001$.

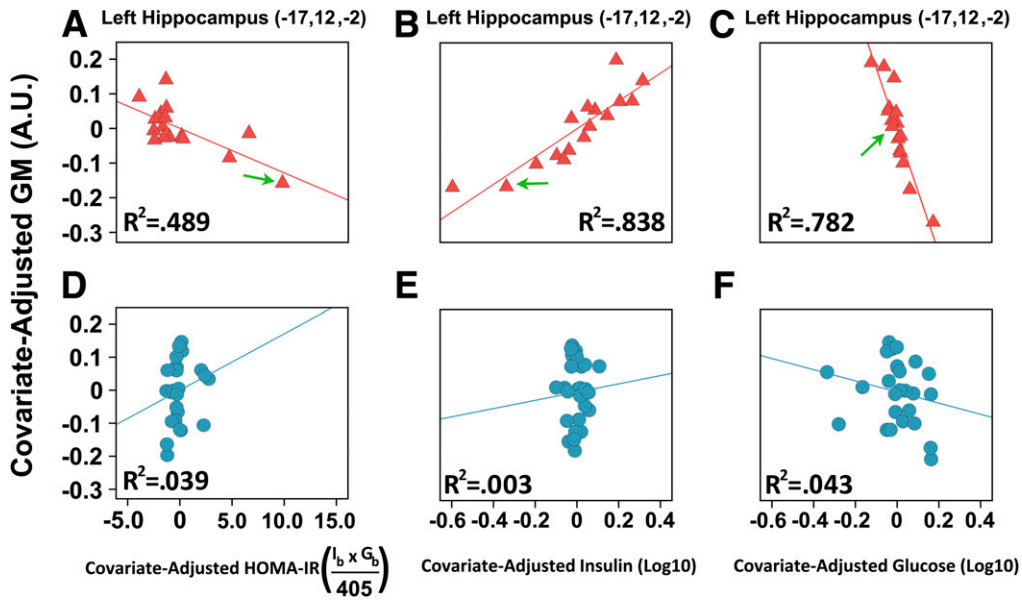

FIG. 2. Partial regression plots depicting error variance of the S_I × dietary condition interaction explained by the HOMA-IR, basal insulin, and basal glucose. Control (n = 16) and CR (n = 26) monkeys are, respectively, represented by red triangles and blue circles. The green arrows indicate a representative control subject across parameters. Among controls, increases in HOMA-IR and basal glucose predicted less GM, whereas higher insulin levels were associated with more GM. These relationships were not significant among CR monkeys. GM volume is depicted in arbitrary units (A.U.).

glucoregulatory dysfunction, brain, and behavior. As S_I increases during CR, there might be less hippocampal atrophy over time that could positively influence task learning and performance. A comparable increase in insulin sensitivity among controls, by contrast, may be detrimental to hippocampus and could negatively affect mMAP performance.

There are several limitations that should be noted. It is not yet clear if improved peripheral insulin signaling in primates reflects similar processes in the brain. It must also be established if the relationship between insulin sensitivity and GM primarily reflects glucose uptake dynamics or other functions of insulin. For controls, the discrepancy between HOMA-IR and S_I findings for GM warrant caution in interpretation, although several measures of insulin sensitivity produced the same result. Given that CR monkeys have less age-related morbidity and mortality (15), there may also be a survivor bias that influenced the voxel-wise results. This bias may make current results more conservative, however, given that surviving controls are likely more resilient to age-related pathophysiology. Regarding mediational models, glucoregulatory variables are sometimes multicollinear and may affect the interpretation of coefficients but not the overall model. Although basal insulin and HOMA-IR were very highly correlated (data not shown), this relationship is sensible both physiologically and statistically. Finally, the existing data are cross-sectional, and causation cannot be inferred.

In summary, increased S_I among CR monkeys was associated with more GM in parietofrontal cortices, hippocampus, and other regions that vary in insulin receptor density and signaling. Among controls, higher S_I showed a positive relationship with GM volume in parietofrontal cortices with low insulin receptor density, but predicted less GM in structures and areas that have high receptor density. CR or CR mimetics may benefit some specific brain regions and aspects of task learning and performance. Nevertheless, additional studies are needed to validate and clarify the association between glucoregulatory dysfunction and GM volume.

ACKNOWLEDGMENTS

This study was supported in part by the National Institutes of Health grants RR-000167, AG-011915, AG-000213, GM-007507, MH-085051, and MH-062015. This study was also supported with resources and facilities at the William S. Middleton Memorial Veterans Hospital. This research was conducted in part at a facility constructed with support from Research Facilities Improvement Program grants RR-15459-01 and RR-020141-01.

No potential conflicts of interest relevant to this article were reported.

A.A.W. researched the data, analyzed the data, and wrote the manuscript. B.B.B., E.K.K., A.S.F., A.L.A., A.S., D.B.A., R.A., and M.-L.V. offered expertise and reviewed and edited the manuscript. J.W.K. researched the glucoregulation data in addition to offering expertise and editing the manuscript. R.J.C., R.H.W., and S.C.J. contributed resources and reviewed and edited the manuscript. S.C.J. is the guarantor of this work and, as such, had full access to all the data in the study and takes responsibility for the integrity of the data and the accuracy of the data analysis.

The authors thank R. Fisher of the University of Wisconsin-Madison and the Waisman Center for Brain Imaging at the University of Wisconsin-Madison for assistance.

REFERENCES

1. Blalock EM, Grondin R, Chen KC, et al. Aging-related gene expression in hippocampus proper compared with dentate gyrus is selectively associated with metabolic syndrome variables in rhesus monkeys. J Neurosci 2010;30:6058–6071
2. Craft S, Watson GS. Insulin and neurodegenerative disease: shared and specific mechanisms. Lancet Neurol 2004;3:169–178
3. Burns JM, Donnelly JE, Anderson HS, et al. Peripheral insulin and brain structure in early Alzheimer disease. Neurology 2007;69:1094–1104

4. Henneberg N, Hoyer S. Short-term or long-term intracerebroventricular (i.c.v.) infusion of insulin exhibits a discrete anabolic effect on cerebral energy metabolism in the rat. Neurosci Lett 1994;175:153–156
5. Mattson MP, Pedersen WA, Duan W, Culmsee C, Camandola S. Cellular and molecular mechanisms underlying perturbed energy metabolism and neuronal degeneration in Alzheimer's and Parkinson's diseases. Ann N Y Acad Sci 1999;893:154–175
6. Liang WS, Reiman EM, Valla J, et al. Alzheimer's disease is associated with reduced expression of energy metabolism genes in posterior cingulate neurons. Proc Natl Acad Sci USA 2008;105:4441–4446
7. Reaven GM. Banting lecture 1988. Role of insulin resistance in human disease. Diabetes 1988;37:1595–1607
8. Schmidt AM, Hori O, Brett J, Yan SD, Wautier JL, Stern D. Cellular receptors for advanced glycation end products. Implications for induction of oxidant stress and cellular dysfunction in the pathogenesis of vascular lesions. Arterioscler Thromb 1994;14:1521–1528
9. Burdo JR, Chen Q, Calcutt NA, Schubert D. The pathological interaction between diabetes and presymptomatic Alzheimer's disease. Neurobiol Aging 2009;30:1910–1917
10. Biessels GJ, van der Heide LP, Kamal A, Bleys RL, Gispen WH. Ageing and diabetes: implications for brain function. Eur J Pharmacol 2002;441:1–14
11. van Harten B, de Leeuw FE, Weinstein HC, Scheltens P, Biessels GJ. Brain imaging in patients with diabetes: a systematic review. Diabetes Care 2006; 29:2539–2548
12. Ashburner J, Friston KJ. Voxel-based morphometry—the methods. Neuroimage 2000;11:805–821
13. Kemnitz JW, Roecker EB, Weindruch R, Elson DF, Baum ST, Bergman RN. Dietary restriction increases insulin sensitivity and lowers blood glucose in rhesus monkeys. Am J Physiol 1994;266:E540–E547
14. Gresl TA, Colman RJ, Roecker EB, et al. Dietary restriction and glucose regulation in aging rhesus monkeys: a follow-up report at 8.5 yr. Am J Physiol Endocrinol Metab 2001;281:E757–E765
15. Colman RJ, Anderson RM, Johnson SC, et al. Caloric restriction delays disease onset and mortality in rhesus monkeys. Science 2009;325: 201–204
16. Bergman RN. Lilly lecture 1989. Toward physiological understanding of glucose tolerance. Minimal-model approach. Diabetes 1989;38:1512–1527
17. Messier C, Teutenberg K. The role of insulin, insulin growth factor, and insulin-degrading enzyme in brain aging and Alzheimer's disease. Neural Plast 2005;12:311–328
18. Duelli R, Schröck H, Kuschinsky W, Hoyer S. Intracerebroventricular injection of streptozotocin induces discrete local changes in cerebral glucose utilization in rats. Int J Dev Neurosci 1994;12:737–743
19. Henneberg N, Hoyer S. Desensitization of the neuronal insulin receptor: a new approach in the etiopathogenesis of late-onset sporadic dementia of the Alzheimer type (SDAT)? Arch Gerontol Geriatr 1995;21:63–74
20. Whitwell JL, Jack CR Jr. Comparisons between Alzheimer disease, frontotemporal lobar degeneration, and normal aging with brain mapping. Top Magn Reson Imaging 2005;16:409–425
21. Rasgon NL, Kenna HA, Wroolie TE, et al. Insulin resistance and hippocampal volume in women at risk for Alzheimer's disease. Neurobiol Aging 2011;32:1942–1948
22. Rezzi S, Martin FP, Shanmuganayagam D, Colman RJ, Nicholson JK, Weindruch R. Metabolic shifts due to long-term caloric restriction revealed in nonhuman primates. Exp Gerontol 2009;44:356–362
23. Kriegeskorte N, Lindquist MA, Nichols TE, Poldrack RA, Vul E. Everything you never wanted to know about circular analysis, but were afraid to ask. J Cereb Blood Flow Metab 2010;30:1551–1557
24. Gash DM, Zhang Z, Umberger G, et al. An automated movement assessment panel for upper limb motor functions in rhesus monkeys and humans. J Neurosci Methods 1999;89:111–117
25. Kastman EK, Willette AA, Coe CL, et al. A calorie-restricted diet decreases brain iron accumulation and preserves motor performance in old rhesus monkeys. J Neurosci 2010;30:7940–7947
26. Gheysen F, Van Opstal F, Roggeman C, Van Waelvelde H, Fias W. Hippocampal contribution to early and later stages of implicit motor sequence learning. Exp Brain Res 2010;202:795–807
27. Ramsey JJ, Colman RJ, Binkley NC, et al. Dietary restriction and aging in rhesus monkeys: the University of Wisconsin study. Exp Gerontol 2000;35: 1131–1149
28. McLaren DG, Kosmatka KJ, Oakes TR, et al. A population-average MRI-based atlas collection of the rhesus macaque. Neuroimage 2009;45:52–59
29. Basser PJ. Inferring microstructural features and the physiological state of tissues from diffusion-weighted images. NMR Biomed 1995;8:333–344
30. Willette AA, Gallagher C, Bendlin BB, McLaren DG, Kastman EK, Canu E, Kosmatka KJ, Field AS, Alexander AL, Colman RJ, et al. Homocysteine, neural atrophy, and the effect of caloric restriction in rhesus monkeys. Neurobiol Aging 2012;33:670–680
31. Ashburner J. A fast diffeomorphic image registration algorithm. Neuroimage 2007;38:95–113
32. Bergman RN, Ider YZ, Bowden CR, Cobelli C. Quantitative estimation of insulin sensitivity. Am J Physiol 1979;236:E667–E677
33. Matthews DR, Hosker JP, Rudenski AS, Naylor BA, Treacher DF, Turner RC. Homeostasis model assessment: insulin resistance and beta-cell function from fasting plasma glucose and insulin concentrations in man. Diabetologia 1985;28:412–419
34. Knickmeyer RC, Styner M, Short SJ, et al. Maturational trajectories of cortical brain development through the pubertal transition: unique species and sex differences in the monkey revealed through structural magnetic resonance imaging. Cereb Cortex 2010;20:1053–1063
35. Saleem KS, Pauls JM, Augath M, et al. Magnetic resonance imaging of neuronal connections in the macaque monkey. Neuron 2002;34:685–700
36. Schmahmann J, Pandya J. *Fiber Pathways of the Brain*. New York, Oxford University Press, 2006
37. Paxinos G, Huang X-F, Toga A. *The Rhesus Monkey Brain in Stereotaxic Coordinates*. Orlando, Academic Press, 2000
38. Unger JW, Livingston JN, Moss AM. Insulin receptors in the central nervous system: localization, signalling mechanisms and functional aspects. Prog Neurobiol 1991;36:343–362
39. McMorris FA, Mozell RL, Carson MJ, Shinar Y, Meyer RD, Marchetti N. Regulation of oligodendrocyte development and central nervous system myelination by insulin-like growth factors. Ann N Y Acad Sci 1993;692:321–334
40. Yau PL, Javier DC, Ryan CM, et al. Preliminary evidence for brain complications in obese adolescents with type 2 diabetes mellitus. Diabetologia 2010;53:2298–2306
41. Salkovic-Petrisic M, Tribl F, Schmidt M, Hoyer S, Riederer P. Alzheimer-like changes in protein kinase B and glycogen synthase kinase-3 in rat frontal cortex and hippocampus after damage to the insulin signalling pathway. J Neurochem 2006;96:1005–1015
42. de la Torre JC. Cerebrovascular and cardiovascular pathology in Alzheimer's disease. Int Rev Neurobiol 2009;84:35–48
43. Reddy KJ, Singh M, Bangit JR, Batsell RR. The role of insulin resistance in the pathogenesis of atherosclerotic cardiovascular disease: an updated review. J Cardiovasc Med (Hagerstown) 2010;11:633–647
44. Orosco M, Rouch C, Gripois D, et al. Effects of insulin on brain monoamine metabolism in the Zucker rat: influence of genotype and age. Psychoneuroendocrinology 1991;16:537–546
45. Stenholm S, Harris TB, Rantanen T, Visser M, Kritchevsky SB, Ferrucci L. Sarcopenic obesity: definition, cause and consequences. Curr Opin Clin Nutr Metab Care 2008;11:693–700
46. Gazdag AC, Sullivan S, Kemnitz JW, Cartee GD. Effect of long-term caloric restriction on GLUT4, phosphatidylinositol-3 kinase p85 subunit, and insulin receptor substrate-1 protein levels in rhesus monkey skeletal muscle. J Gerontol A Biol Sci Med Sci 2000;55:B44–B446; discussion B47–B48.
47. Anson RM, Guo Z, de Cabo R, et al. Intermittent fasting dissociates beneficial effects of dietary restriction on glucose metabolism and neuronal resistance to injury from calorie intake. Proc Natl Acad Sci USA 2003;100: 6216–6220